http://dx.doi.org/10.5012/bkcs.2012.33.10.3218

One Pot Synthesis and Characterization of Alginate Stabilized Semiconductor Nanoparticles

Parani Sundarrajan, Prabakaran Eswaran, Alexander Marimuthu, Lakshmi Baddireddi Subhadra,† and Pandian Kannaiyan*

Department of Inorganic Chemistry, University of Madras, Maraimalai (Guindy) Campus, Chennai-600 025, India
**E-mail: chem.pandian@yahoo.in*
†*Tissue Culture and Drug Discovery Laboratory, Centre for Biotechnology, Anna University, Chennai-600 025, India*
Received May 30, 2012, Accepted July 5, 2012

Uniform and well dispersed metal sulfide semiconductor nanoparticles incorporated into matrices of alginate biopolymer are prepared by using a facile *in situ* method. The reaction was accomplished by impregnation of alginate with divalent metal ions followed by reaction with thioacetamide. XRD analysis showed that the nanoparticles incorporated in the polymer matrix were of cubic structure with the average particle diameter of 1.8 to 4.8 nm. Field emission scanning electron microscopy and high resolution transmission electron microscopy images indicated that the particles were well dispersed and distributed uniformly in the matrices of alginate polymer. FT-IR spectra confirmed the presence of alginate in the nanocomposite. The crystalline nature and thermal stability of the alginate polymer was found to be influenced by the nature of the divalent metal ions used for the synthesis. The proposed method is considered to be a simple and greener approach for large scale synthesis of uniform sized nanoparticles.

Key Words : Biopolymers, Alginate, Ion exchange, Semiconductor nanoparticles

Introduction

Semiconductor nanoparticles stabilized by a polymeric backbone have been synthesized over the past decade due to their excellent mechanical, optical, optoelectronic properties[1-4] and vital applications in laser optics,[5] solar cells[6] and sensor devices.[7] Polymers are well known for their optical transparency, physical and chemical stability, tunable mechanical properties and easy molding. In addition to these, biopolymers have an additional advantage compared with synthetic polymers, as they are readily available, biodegradable, biocompatible and nontoxic to the environment. A variety of biopolymers such as protein, nucleic acid and polysaccharides have been employed as stabilizing agent for both metal and semiconductor nanoparticles. The carboxyl and hydroxyl groups present in these polymers form a complex with metal ions and provide a good environment for controlled growth of nanoparticles within the polymer network. Based on this, biopolymers such as DNA,[8,9] chitosan,[10] starch,[11] dextran[12] and gelatin[13,14] have been used to stabilize nanoparticles of metal and semiconductors. However only few articles had been reported in the literature on alginate stabilized nanoparticles. Anh *et al.*,[15] and Jaouen *et al.*,[16] reported the synthesis of Au-alginate bionanocomposite. Recently, Wang *et al.*,[17] and Bardajee *et al.*,[18] have synthesized quantum dot encapsulated with alginate by ligand exchange process. Nevertheless, they also used Tri-*n*-octylphosphine oxide or thioglycerol as capping agent which are toxic and pollute the environment. For this reason, it is desirable to use eco-friendly and greener methods to synthesize nanomaterials.

We have chosen sodium alginate (Alg) as the stabilizing agent for the synthesis of semiconductor nanoparticles (ZnS, CdS, PbS) in a single pot method. Alginate, sodium salt of alginic acid is a naturally occurring, totally biodegradable, inexpensive polymer extracted from brown seaweed. It contains hydrophilic, anionic linear homopolysaccharide composed of alternating blocks of 1-4 linked α-L-guluronate and β-D-mannuronate residues.[19,20] It has been utilized for a variety of applications including textile, food, chemical and medical industries. It is also shown to be a promising material and widely exploited in pharmaceutical industry especially in controlled drug release[21] because of its inherent gelation nature,[22] biocompatibility, bio adhesiveness, low toxicity and pH sensitivity.[23,24]

In this report, a single pot method was employed to synthesize alginate stabilized metal sulfide semiconductor (Alg-ZnS, Alg-CdS and Alg-PbS) nanoparticles by *in situ* The main idea of this method is based upon the exchange of Na^+ in sodium alginate with divalent metal ions Zn^{2+}, Cd^{2+} and Pb^{2+} followed by incorporation of sulfide ion under refluxing condition to form semiconductor nanoparticles. The as synthesized nanoparticles were characterized by UV-Visible (UV-Vis) and photoluminescence (PL) spectroscopy, FT-IR, FE-SEM, HRTEM, thermo gravimetric analysis (TGA) and XRD techniques. Such alginate stabilized semiconductor nanoparticles can be exploited for biological cell imaging and drug delivery as these nanoparticles (particularly ZnS nanoparticles, because of its low toxicity) act as a fluorescent probe for cell detection and also enhance the drug encapsulation efficiency of alginate.[25] Other possible applications include sensing[26] and photocatalysis.[27]

Experimental Section

Materials. Cadmium nitrate tetrahydrate $Cd(NO_3)_2 \cdot 4H_2O$, lead nitrate $Pb(NO_3)_2$, zinc acetate dihydrate $Zn(CH_3COO)_2 \cdot 2H_2O$ were purchased from Merck, India. Thioacetamide and sodium alginate were purchased from SRL, India. All chemicals were of analar grade and used as received. Double distilled water was used for synthesis and all optical measurements.

Instruments. UV-Vis absorption spectra were recorded with a Shimadzu, (Model UV-1800) UV-Visible spectrophotometer, Japan. For Near IR (NIR) absorption spectral studies, Cary-5E UV-Vis-NIR Spectrophotometer, USA was used. PL measurements were performed using a Perkin-Elmer LS 5B, USA Spectrofluorimeter instrument. FT-IR spectra of the samples were recorded using a Perkin-Elmer, USA (Model Y 40) within the range of 4000-400 cm^{-1}. XRD patterns of the samples were recorded by using Brucker D8 Advance diffractometer with monochromatic Cu-Kα_1 radiation (λ = 1.5418 Å). The morphology of the polymeric composite films was analyzed with FE-SEM instrument (Hitachi Ltd., SU6600, Japan). HRTEM images were obtained from a FEI Tecnai G^2 (T-30) with an operating voltage of 250 kV. Samples for TEM analysis were ultrasonicated in ethanol for few minutes and the drop of dispersion was coated on carbon coated copper grids. Thermogravimetric (TGA) analysis was conducted using TGA Q500 V6.7 Build 203 thermal analyzer.

Synthesis of Alginate Stabilized Metal Sulfide Semiconductor Nanoparticles (Alg-MS). In a typical synthesis, a known amount of metal salts (10 mL, 0.1 M) was added to an aqueous solution of sodium alginate (20 mL, 1%). The reaction mixture was allowed to stir for 30 min at room temperature followed by the addition of an equimolar volume of thioacetamide. The mixture was then heated to reflux at 100 ºC for about 1 h. The resulting products were isolated by filtration followed by extensive washing with water and dried under vacuum at room temperature.

Results and Discussion

Synthesis. Synthesis of alginate stabilized semiconductor nanoparticles can be described as follows: (1) preparation of sodium alginate sol; (2) gel transformation of alginate sol by diffusion and complexation with divalent cations leading to network cross-linking; (3) formation of semiconductor nanoparticles by incorporation of sulfide ion at refluxing condition (Scheme 1). The ion exchange of Na^+ in sodium alginate by Zn^{2+}, Cd^{2+} or Pb^{2+} metal ions (M^{2+}) was carried out at room temperature. These divalent metal ions show high affinity to alginates rich in polyguluronate units.[28] The process of ion exchange transforms the alginate from sol to gel through ionic crosslinking of M^{2+} with alginate chain molecules.

The metal ions are ionically substituted at the carboxylic site of polyguluronate units and fit into electronegative cavities, like eggs in egg box forming a linked alginate strands.[29]

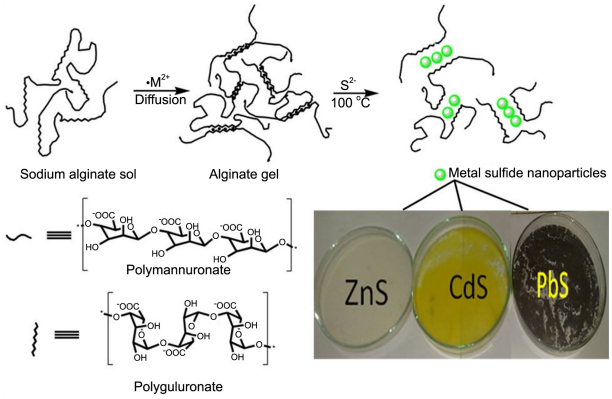

Scheme 1. Schematic representation of synthesis of Alg-MS nanoparticles. The *inset* shows the digital photograph of ZnS, CdS, PbS nanoparticles in alginate matrix.

The gel formation is also accompanied by the generation of capillaries or channel like pores due to the directed diffusion of metal ions in a broad front with a certain propagation velocity from one direction into the alginate sol.[30] Generation of such capillaries is observed from FE-SEM image (see, Figure S1 in supporting information). The capillaries are almost uniform in diameter and show parallel alignment and equally spaced. In the presence of sulfide ion (S^{2-}) released from the aqueous solution of thioacetamide, nucleation of monomers takes place inside the three dimensional network of the polymer[31] by the interaction of divalent metal ions (M^{2+}) coordinated to carboxylic acid groups in the alginate polymer with the sulfide ion. The monomers aggregate further into nanoparticles which can easily be identified from their colors. Alg-ZnS and Alg-CdS nanoparticles impart white and yellow colors to the alginate matrix whereas the Alg-PbS nanoparticles depict black color to the gel. The optical images of the products after drying at room temperature are shown in inset in Scheme 1. Upon formation of nanoparticles, a decrease in solution viscosity (gelation) is observed as reported earlier.[16] This is due to that, with introduction of S^{2-} in the gel, new bond between M-S is formed and hence the interaction between the M^{2+} and alginate decreases leading to decrease in solution viscosity.

Optical Studies. The aqueous solution of sodium alginate itself has an absorption band around 260 nm (see, Figure S2 in supporting information). It can be assigned to double bonds of alginate formed after main chain scission of the polymer.[32] With the addition of metal salts, a band around 300 nm is appeared in the spectra indicating the formation of Alg-M^{2+} complex (Figure S2). After the addition of S^{2-} which is released by thermal decomposition of aqueous solution of thioacetamide,[8] to the Alg-M^{2+} complex, Alg-MS nanoparticles were formed and the absorption peak at 260 nm (Figure 1) becomes very strong. This suggests that the scission of the alginate molecule takes place strongly after the formation of nanoparticles within the polymer matrix. Besides, Alg-ZnS nanoparticles exhibit a shoulder band in the UV region below 320 nm (Figure 1(a)) whereas Alg-CdS nanoparticles show a characteristic absorption shoulder peak

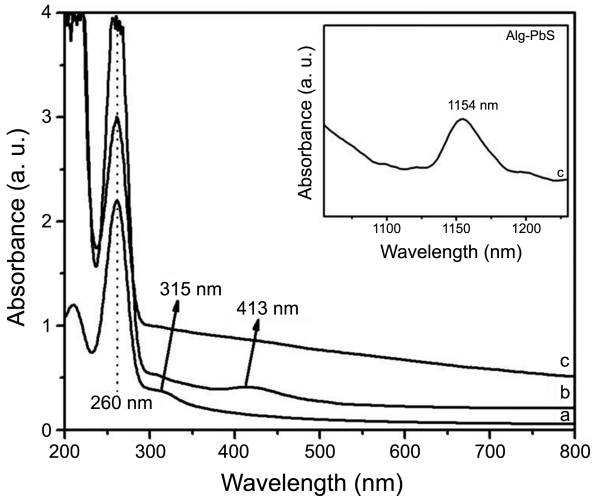

Figure 1. UV-Visible spectrum of (a) Alg-ZnS, (b) Alg-CdS and (c) Alg-PbS nanoparticles. The *inset* shows the absorption spectrum of Alg-PbS in NIR region.

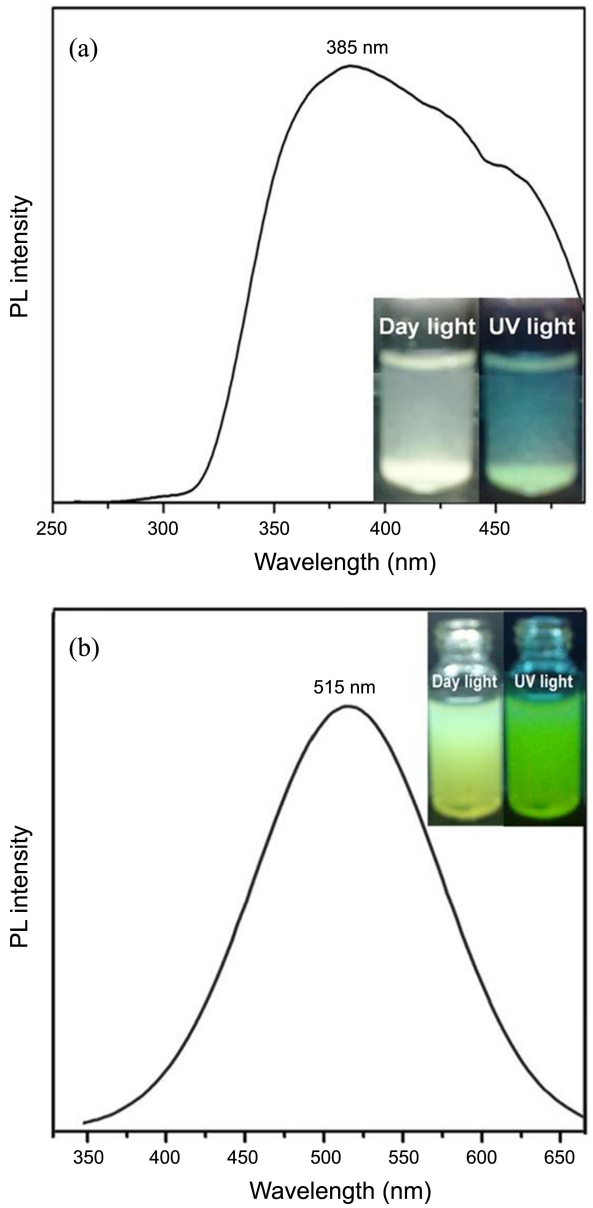

Figure 2. PL spectrum of (a) Alg-ZnS (λ_{ex} = 250 nm) and (b) Alg-CdS (λ_{ex}= 340 nm).The *insets* shows the digital photographs of the samples under day light and UV light.

at 413 nm in visible region (Figure 1(b)) and Alg-PbS nanoparticles show at 1154 nm in the NIR region (Figure 1 inset). UV-Vis absorption spectrum of all Alg-MS nanoparticles, when compared to their bulk MS, show the characteristic blue shift. These results indicate the quantum confinement of semiconductor nanoparticles within the alginate polymer matrix.[33] The alginate chains cause electrostatic repulsion between nanoparticles and also kept them apart sterically because of its chain length, which is also used to explain the quantum confinement. The emission spectrum of Alg-ZnS and Alg-CdS are shown in Figure 2(a) and Figure 2(b). Alg-ZnS shows blue emission (Figure 2(a) Inset) with emission maximum at 385 nm and Alg-CdS shows green emission (Figure 2(b) Inset) at 515 nm. The emission peaks are broader with the full-width half-maximum of 147 nm for Alg-ZnS and 140 nm for Alg-CdS. These broad emissions are attributable to more polar medium of semiconductors due to the presence of polysaccharide backbones.[18] The other reason can be attributed to charge carrier recombination in trap states due to surface defects.[34]

FT-IR Analysis. FT-IR spectrum of sodium alginate and Alg-MS nanoparticles are shown in Figure 3 and the assignments of some of the most characteristic vibrational modes are given in Table S1 in supporting information. The -OH group present in sodium alginate (Figure 3(a)) exhibits a broad band around 3400 cm^{-1}. The peaks attributed to the -CH_2 groups are present at 2925 cm^{-1} and 2857 cm^{-1}. The bands around 1030 cm^{-1} present in the spectrum of sodium alginate are attributed to its saccharide structure (C-O-C stretching). In addition, the bands at 1621 cm^{-1} and 1417 cm^{-1} are assigned to asymmetric and symmetric stretching peaks of carboxylate salt groups.[35] All the above peaks are also observed in the case of Alg-MS nanoparticles. As seen in the figure, it is clearly observed that there is a large shift ~30 cm^{-1} to lower wavenumber for the peaks assigned to symmetric stretching of carboxylate salt groups in the spectra of Alg-CdS (Figure 3(c)) and Alg-PbS (Figure 3(d)) while the that of Alg-ZnS (Figure 3(b)) shows little shift ~7 cm^{-1}. This might be due to the different binding capacity of alginates with metal species arising from metal acetate or metal nitrate salts. The peaks in the spectra of Alg-MS are also sharper than those of sodium alginate. This reflects the limited mobility of semiconductor nanoparticles fixed by the guluronate units of sodium alginate, which produces hidden peaks compared to those of sodium alginate.[36] These interesting changes indicate the fact that carboxylate groups have some interaction with semiconductor nanoparticles. However, the characteristic vibration of the M-S bond of Alg-MS cannot be detected or merged with alginate peaks in the FTIR spectrum.

XRD Analysis. Figure 4 represents the XRD patterns of sodium alginate and Alg-MS nanoparticles. Sodium alginate

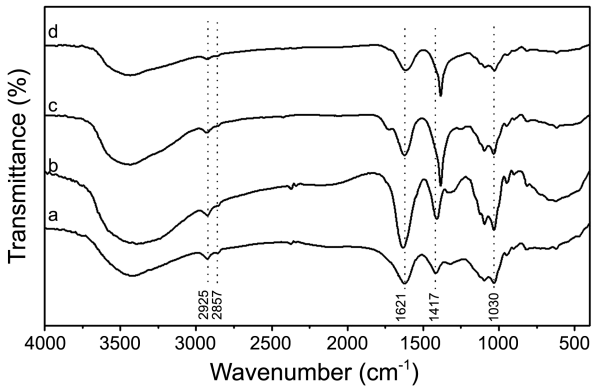

Figure 3. FT-IR spectra of (a) sodium alginate, (b) Alg-ZnS, (c) Alg-CdS and (d) Alg-PbS nanoparticles.

is usually crystalline due to strong interaction between the alginate chains through intermolecular hydrogen bonding.[37] Three diffraction peaks at 2θ values 13.5º, 22º and 39º were observed for sodium alginate (Figure 4(a)) due to the reflection of their (110) plane from polyguluronate unit, (200) plane from polymannuronate and the other from amorphous halo.[38] In case of Alg-MS, the intensity of diffraction peaks of alginate decreased notably which indicates that the nucleation and growth of semiconductor nanoparticles affected the crystalline nature of sodium alginate. Apart from these, three major diffraction peaks were observed in the XRD pattern of Alg-ZnS (Figure 4(b)) and Alg-CdS (Figure 4(c)) which is due to reflection of their (111), (220), and (311) planes whereas Alg-PbS (Figure 4(d)) shows six major diffraction peaks due to reflections from the (111), (200), (220), (311), (222), (420) and (422) planes. For all samples, the peak positions are attributed to cubic structures and matched with the JCPDS cards (ZnS JCPDS card no. 80-0020, CdS, JCPDS card no. 42-1411 and PbS, JCPDS card no. 78-1901). The broadening of the diffraction peaks in all three cases indicates nanoparticle nature of the sample. The average crystallite sizes were determined from the line width of all diffraction peaks using Debye-Scherrer formula ($d = 0.9\lambda/\beta \cos(\theta)$ where d is the diameter of the particle, λ is the wavelength of the X-ray used, β is the full width at half maximum and θ is the scattering angle). In order to determine β, the peak profile was obtained by fitting observed diffraction patterns with Gaussian curves. The calculation yields an average crystallite size of 1.8 nm, 2.7 nm and 4.8 nm in diameter for Alg-ZnS, Alg-CdS and Alg-PbS nanoparticles respectively.

FE-SEM and HRTEM Analysis. The shape and size of the samples were investigated using FE-SEM and HRTEM analysis. Figure 5 shows FE-SEM images of Alg-ZnS (Figure 5(a)), Alg-CdS (Figure 5(b)) and Alg-PbS (Figure 5(c)) nanoparticles. It is seen that the lot of polymer composite nanoparticles are agglomerated with spherical shape and distributed in a compact manner within the film. EDAX

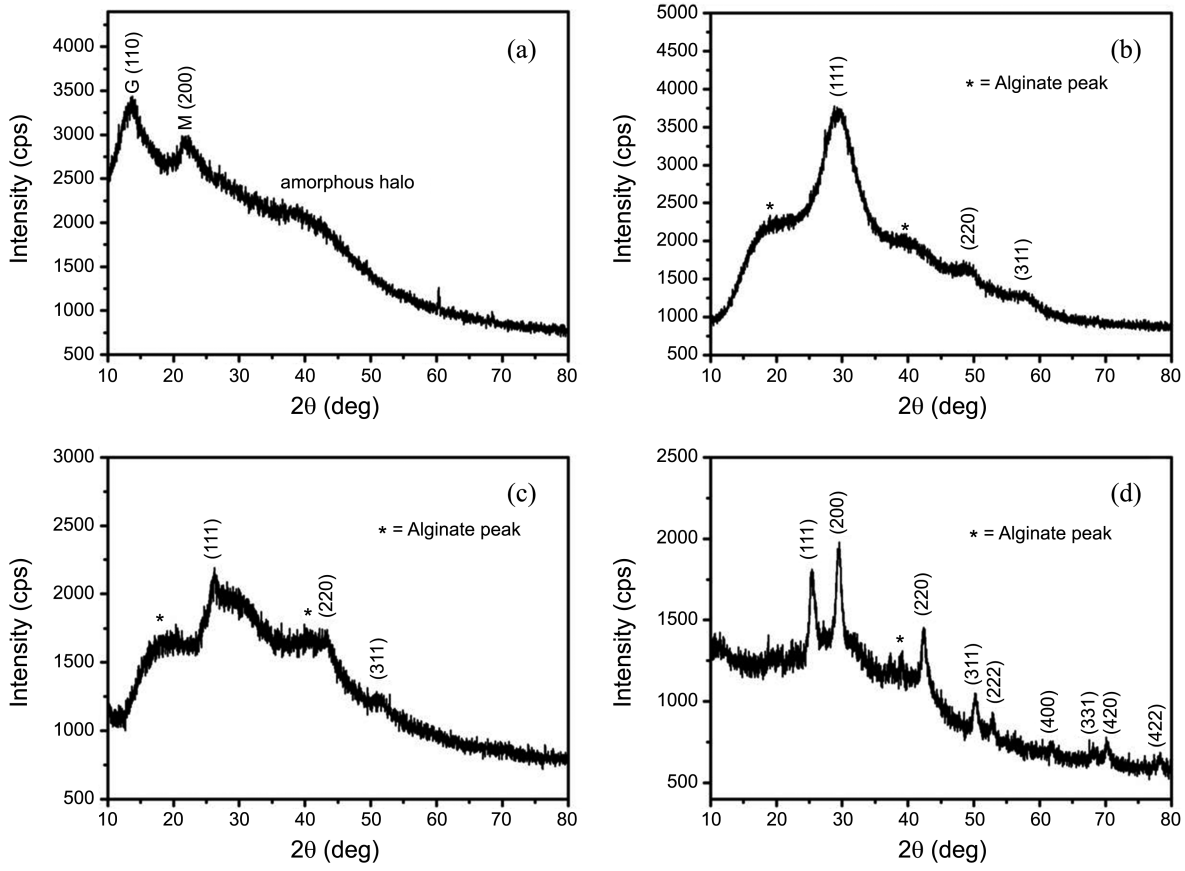

Figure 4. XRD patterns of (a) sodium alginate, (b) Alg-ZnS, (c) Alg-CdS and (d) Alg-PbS nanoparticles.

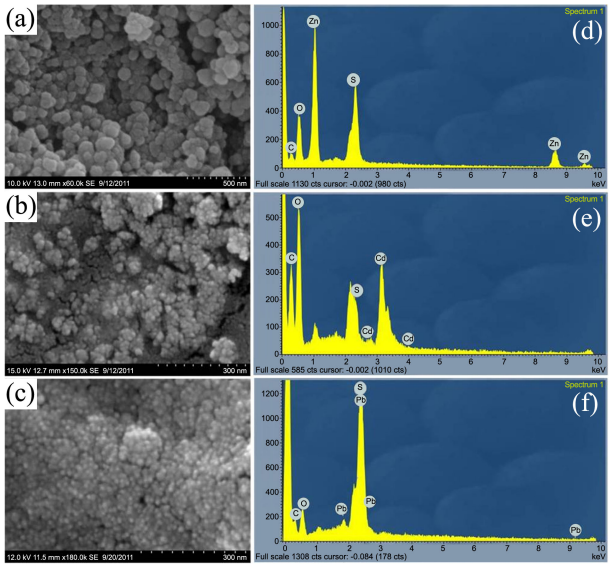

Figure 5. FE-SEM images (a) Alg-ZnS, (b) Alg-CdS, and (c) Alg-PbS nanoparticles and their corresponding EDAX analysis on their right side (d-f).

spectra of the composite films clearly show the characteristic peaks of metals and sulfur used for the synthesis along with notable amounts of carbon and oxygen from alginate backbone. The obtained nanocmposites were further characterized by HRTEM. Figure 6 shows the TEM images of Alg-ZnS (Figure 6(a)), Alg-CdS (Figure 6(b)) and Alg-PbS (Figure 6(c)) nanoparticles. The composite film consists of fine dispersion of semiconductor nanoparticles throughout alginate matrix which can be seen in light contrast when compared with the electron dense metal sulfide nanoparticles. The particle size calculated from histograms of TEM measurements (Figure 6(d)-(f)) was found to be almost same with the results from XRD measurements.

Thermal Studies. Figure 7 illustrates TGA and differential TGA (DTG) curves of pure alginate and Alg-MS nanocomposite. TGA shows the onset of decomposition near 60 ºC which is due to the loss of water molecules trapped in the samples. Sodium alginate shows the principle weight loss between 205 ºC to 285 ºC with a maximum at 265 ºC (Figure 7(a)) corresponding to the complete decomposition of its alginate backbone structure. Incorporation of ZnS and CdS (Figure 7(b) and 7(c)) in the alginate matrices increases the polymer decomposition temperature (280 ºC) while incorporation of PbS (Figure 7(d)) greatly decreases (almost 40% of the polymer was decomposed at 250 ºC). There are numerous reports which state that incorporation of inorganic materials in the polymer matrix usually increases the thermal stability of the polymer.[39-41] Contradictory result was obtained by Wang *et al*..[42] Earlier it was reported that various factors such as gel formation, ion exchange, and affinity towards alginate depended on the nature of the divalent metal ions and varied in the order Pb^{2+}, Cd^{2+}, Zn^{2+} or *vice versa*.[28] We also have observed the same trend in crystalline degree and thermal stability by XRD and TGA analysis (see, Figure S3 in supporting information). It is observed from XRD patterns that the intensity of alginate peaks in Alg-PbS is very low when compared to that of alginate peaks in Alg-CdS and Alg-ZnS. This could be due to the interactions between MS with sodium alginate decrease the intermolecular interaction between the alginate chains in the order Pb

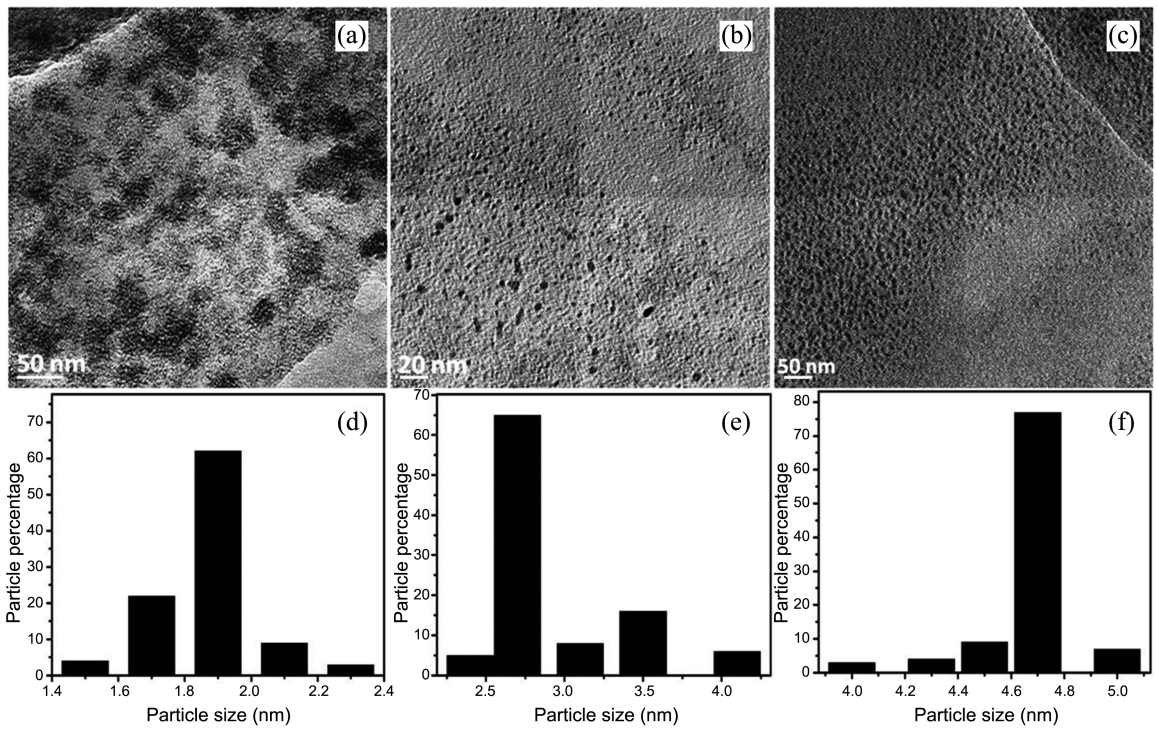

Figure 6. HRTEM images of (a) Alg-ZnS, (b) Alg-CdS, and (c) Alg-PbS nanoparticles and their representative diameter-distribution histograms at their bottom (d-f).

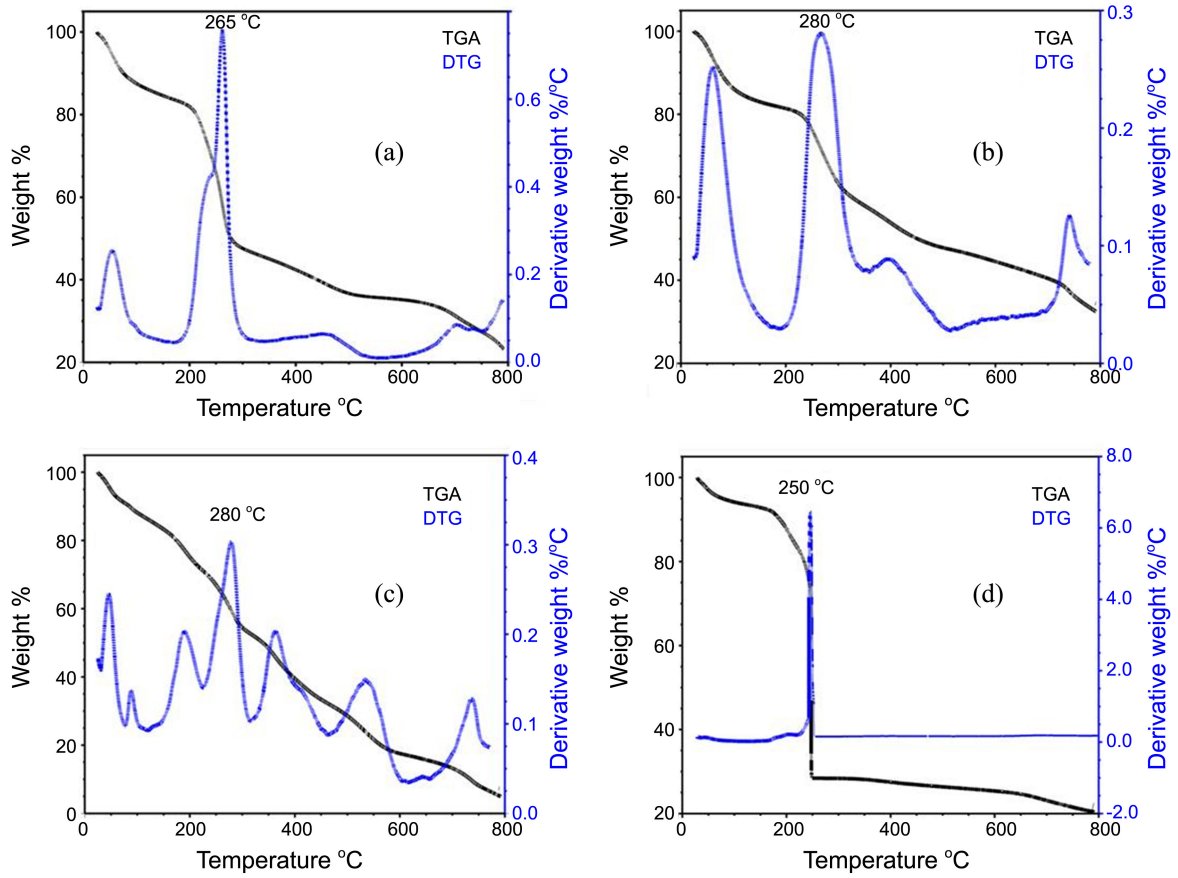

Figure 7. TGA/DTG plot for the thermal behavior of (a) sodium alginate, (b) Alg-ZnS, (c) Alg-CdS and (d) Alg-PbS nanoparticles.

> Cd > Zn and thus the crystalline degree, thermal stability of alginate is depressed. TG curves then show a further weight loss due to decomposition of metal sulfides to metal oxides and oxysulfates.[12]

Conclusion

In summary, we have developed a simple method for the synthesis of alginate stabilized metal sulfide semiconductor nanoparticles by exchange of Na^+ ion in alginate with divalent metal ions followed by the incorporation of sulfide ion. The formation of semiconductor nanoparticles within the alginate matrix was confirmed by UV-Vis, FT-IR, XRD, FE-SEM and HRTEM studies. The as synthesized nanoparticles have cubic structures according to XRD patterns. The nanoparticles were uniformly distributed in the alginate polymer. The thermal stability and crystalline nature of Alg-MS nanoparticles was compared with that of pure sodium alginate and it depends on the nature of the divalent metal ions used for the synthesis. This method is considered to be simple, cheap and green method for synthesis of semiconductor nanoparticles for wide range of applications such as metal ion sensing cancer cell imaging and catalysis.

Acknowledgments. The authors (K.P. and B.S.L) express their gratitude to the Department of Biotechnology (DBT-Nanomedicine), New Delhi, Government of India for providing financial support (Grant No: BT/PR10085/NNT/28/99/2007) to carry out a part of this work. The authors also acknowledge the assistance from National Centre for Nanoscience and Nanotechnology, University of Madras for providing FE-SEM, HRTEM and XRD facilities. We express here our sincere thanks to M/s Orchid Chemicals and Pharmaceuticals Ltd, Chennai, Tamilnadu for providing TGA facility and SAIF, IIT Madras for NIR absorption spectral studies.

References

1. Caseri, W. *Macromol. Rapid. Commun.* **2000**, *21*, 705.
2. Beecroft, L. L.; Ober, C. K. *Chem. Mater.* **1997**, *9*, 1302.
3. Sun, Y. P.; Rollins, H. *Chem. Phys. Lett.* **1998**, *288*, 585.
4. Wang, M.; Zhang, M.; Qian, J.; Zhao, F.; Shen, L.; Scholes, G. D.; Winnik, M. A. *Langmuir* **2009**, *25*, 11732.
5. Hoogland, S.; Sukhovatkin, V.; Howard, I.; Cauchi, S.; Levina, L.; Sargent, E. H. *Opt. Express* **2006**, *14*, 3273.
6. Huynh, W. U.; Dittmer, J. J.; Alivisatos, A. P. *Science* **2002**, *295*, 2425.
7. Rajesh; Ahuja, T.; Kumar, D. *Sens. Act. B* **2009**, *136*, 275.
8. Kundu, S.; Lee, H.; Liang, H. *Inorg. Chem.* **2009**, *48*, 121.
9. Ma, N.; Yang, J.; Stewart, K. M.; Kelley, S. O. *Langmuir* **2007**, *23*, 12783.
10. Li, Z.; Du, Y.; Zhang, Z.; Pang, D. *React. Funct. Polym.* **2003**, *55*, 35.

11. Oluwafemi, O. S.; Adeyemi, O. O. *Mater. Lett.* **2010**, *64*, 2310.
12. Kim, Y. Y.; Walsh, D. *Nanoscale* **2010**, *2*, 240.
13. Byrne, S. J.; Williams, Y.; Davies, A.; Corr, S. A.; Rakovich, A.; Gun'ko, Y. K.; Rakovich, Y. P.; Donegan, J. F.; Volkov, Y. *Small* **2007**, *3*, 1152.
14. Mozafari, M.; Moztarzadeh, F. *J. Colloid. Interface. Sci.* **2010**, *351*, 442.
15. Anh, N. T.; Phu, D. V.; Duy, N. N.; Du, B. D.; Hien, N. Q. *Radiat. Phys. Chem.* **2010**, *79*, 405.
16. Jaouen, V.; Brayner, R.; Lantiat, D.; Steunou, N.; Coradin, T. *Nanotechnology* **2010**, *21*, 185605.
17. Wang, C. H.; Hsu, Y. S.; Peng, C. A. *Biosens. Bioelectron* **2008**, *24*, 1012.
18. Bardajee, G. R.; Hooshyar, Z.; Rostami, I. *Colloids. Surf. B* **2011**, *88*, 202.
19. Gacesa, P. *Carbohydr. Polym.* **1988**, *8*, 161.
20. Guiseley, K. B. *Enzyme. Microb. Technol.* **1989**, *11*, 706.
21. Rangaraj, G.; Kishore, N.; Dhanalekshmi, U. M.; Raja, M. D.; Senthilkumar, C.; Reddy, P. N. *J. Pharm. Sci. Res.* **2010**, *2*, 77.
22. Li, P.; Dai, Y. N.; Zhang, J. P.; Wang, A. Q.; Wei, Q. *Int. J. Biomed. Sci.* **2008**, *4*, 221.
23. Chenoweth, M. B. *Ann. Surg.* **1948**, *127*, 1173.
24. Shilpa, A.; Agrawal, S. S.; Ray, A. R. *J. Macromol. Sci. Polym. Rev.* **2003**, *43*, 187.
25. Li, Z.; Chen, P.; Xu, X.; Ye, X.; Wang, J. *Mater. Sci. Eng. C* **2009**, *29*, 2250.
26. Lai, S.; Chang, X.; Fu, C. *Microchim. Acta* **2009**, *165*, 39.
27. Jiang, R.; Zhu, H.; Li, X.; Xiao, L. *Chem. Eng. J.* **2009**, *152*, 537.
28. Haug, A. *Acta. Chem. Scand.* **1961**, *15*, 1794.
29. Grant, G. T.; Morris, E. R.; Rees, D. A.; Smith, P. J. C.; Thom, D. *FEBS Lett.* **1973**, *32*, 195.
30. Treml, H.; Woelki, S.; Kohler, H. H. *Chem. Phys.* **2003**, *293*, 341.
31. Luccio, T. D.; Laera, A. M.; Tapfer, L. *J. Phys. Chem. B* **2006**, *110*, 12603.
32. Nagasawa, N.; Mitomo, H.; Yoshii, F.; Kume, T. *Polym. Degrad. Stab.* **2000**, *69*, 279.
33. Bhattacharjee, B.; Ganguli, D.; Chaudhuri, S. *J. Nanopart. Res.* **2002**, *4*, 225.
34. Pinna, N.; Weiss, K.; Urban, J.; Pileni, M. P. *Adv. Mater.* **2001**, *13*, 261.
35. Sartori, C.; Finch, D. S.; Ralph, B. *Polymer* **1997**, *38*, 43.
36. Sakugawa, K.; Ikeda, A.; Takemura, A.; Ono, H. *J. Appl. Polym. Sci.* **2004**, *93*, 1372.
37. Fang, D.; Liu, Y.; Jiang, S.; Nie, J.; Ma, G. *Carbohydr. Polym.* **2011**, *85*, 276.
38. Fabia, J.; Slusarczyk, C. Z.; Gawlowski, A. *Fibres. Text. East Eur.* **2005**, *13*, 114.
39. Li, Y.; Liu, E. C. Y.; Pickett, N.; Skabara, P. J.; Cummins, S. S.; Ryley, S.; Sutherland, A. J.; O'Brien, P. *J. Mater. Chem.* **2005**, *12*, 1238.
40. Trandafilovic, L. V.; Djoković, V.; Bibic, N.; Georges, M. K.; Radhakrishnan, T. *Opt. Materials* **2008**, *30*, 1208.
41. Radhakrishnan, T.; Georges, M. K.; Nair, P. S.; Luyt, A. S.; Djoković, V. *Colloid Polym. Sci*. **2008**, *286*, 683.
42. Wang, H.; Fang, P.; Chen, Z.; Wang, S. *Appl. Surf. Sci.* **2007**, *253*, 8495.